THE CONSEQUENCE OF DOPANT ON THE MAGNETIC PROPERTIES OF M-TYPE HEXAFERRITE

Salisu I. Kunya[1], Yunusa Abdu[2], J. Mohammed[3], Mohd Kamarulzaki Mustafa[4] and Mohd Khairul Ahmad[5]

[1]Department of Science laboratory Technology, Jigawa State Polytechnics, Dutse, Nigeria
[2]Department of Physics, Faculty of Physical Sciences, College of Natural and Pharmaceutical Sciences, Bayero University, Kano, Nigeria
[3]Department of Physics, Faculty of Science, Federal University Dutse, P.M.B. 7156, Dutse, Jigawa state, Nigeria
[4]Department of Physics and Chemistry, Faculty of Applied Sciences and Technology, Universiti Tun Hussein Onn Malaysia (UTHM), Kampus Pagoh, Jalan Panchor 84000 Muar, Johor, Malaysia
[5]Microelectronic and Nanotechnology, Shamsuddin Research Centre (MiNT-SRC), Faculty of Electrical and Electronic Engineering, Universiti Tun Hussein Onn Malaysia (UTHM), Parit Raja, Batu Pahat Johor, 86400, Malaysia
Corresponding Author: Salisu I. Kunya, E-mail: salisukunya2016@sgmail com

ABSTRACT

Hexaferrite enhancement is heavily inspired by its cation distribution, particle size, synthesis method, and morphology. Cation doping is thus among the most useful ways to enhance the magnetic properties of ferrite. The paper provides an overview of M-type hexaferrite and the Sol-gel auto-combustion synthesis technique. The review of the effect of the dopant on the material was investigated. From the hysteresis curve, the magnetic parametres were calculated. For all samples, coercivity, and crystalline anisotropy increase as dopant concentration increases, whereas remanence magnetization decreases. All of the samples' magnetic properties have coercivity greater than 600Oe, implying that the produced materials can be favorable for high-density recording media applications, switching, and high-frequency applications.

Keywords: Dopant, Hexaferrite, M-ferrite, Sol-gel.

1. Introduction

The current research focuses on improving existing materials and synthesizing new materials with excellent properties. Although bulk materials have consistent unique properties regardless of dimension, size-dependent attributes are frequently observed at the nanoscale. Thus, as a material's size approaches the nanoscale its properties change (Singh et al., 2016). The synthesis of ferrite nanomaterials is one of the fascinating research topics (FNMs). The goal is to find the best techniques for making FNMs that are well-structured, crystalline in nature, and have augmented physical characteristics. (Kesavan et al., 2022). A hard permanent magnet item is a material that is highly resistant to demagnetizing fields. As an outcome, coercivity is often used to distinguish between hard or soft ferrites. The coercivity of strong magnetic assets is greater than 125Oe. Permanent magnets are a type of magnetic stronger material. They are employed in order to create a magnetic field. When the specimen is first 'charged,' it stores the energy required to keep the magnetic field. Ceramic ("oxide") magnets are of this type. It is an important part of the present life, but we are often unaware of how many various varieties of these substances we use on a daily basis. The typical applications of these modern material, based upon the energy density $(B.H)_{max}$. Ferrites are an unavoidable part of modern science and technology. Ferrites are unusual and precious ceramic materials that are dark grey or black (Kaur and Bhargava, 2020). They are unusual and useful ceramic materials that are incredibly stiff and strong. They are chemically stable and inexpensive magnetic materials (Khan et al., 2022). In nature, ferrites may be found in many various forms, such as iron (III) oxide (FeO), maghemite $(\gamma - Fe_2O_3)$, and haematite $(\alpha - Fe_2O_3)$. The most prevalent, naturally occurring, and powerful magnetic substance on Earth is magnetite/lodestone (Fe_3O_4) (Harrison et al., 2002). The Chinese used lodestones for the initial time in the twelfth century.

Rather than obeying the stars, it served as a guiding tool and was used by seamen for simple North selection. Ferrites were not the subject of any research before the 1930s. In 1933, Japanese professors Takeshi Takei and Kato were the first to recognize the potential benefits of ferrites' characteristics. Hard and soft ferrites were thereafter produced in large quantities and sold commercially (Mathews and Babu, 2021).

Ferrites have improved magnetic properties, making them useful for a number of applications, including permanent magnets, microwave absorption, and magnetic data recording and storage (Auwal et al., 2016), (Almessiere et al., 2021). Static and dynamic devices are the two categories into which the devices that utilize magnets are divided. Devices that move as a result of a permanent magnet and current interaction are referred to as dynamic devices. As a result, this categorization covers all spinning or linear engines, systems are basically, etc. This category also contains electromagnets for diskettes and optical disk drives, which are now the most significant commercial use. The basic idea behind magnetic recording technology, which has existed for and over a century, is to use a magnetic framework (as the "write" head) motivated by a current that corresponds to the information to be documented to create a magnetic flux capable of changing the state of magnetic properties in a tightly packed magnetic medium. This medium, which was once a magnetic wire but is now recognized as tape or a permanent magnet layered hard drive, was once a magnetic wire but has since changed to become a magnetic medium. Magnetic storage space has experienced a linear growth in storing potential. The foundation of electromagnetic hard disk drive technologies now and in the future is magnetic nanostructure physics. On the basis of their shape, structural features, magnetism, optical, and electrical properties, new magnetic particles are created and employed every year. Depending on how they are to be used (Almessiere et al., 2021). It is frequently utilized because of its numerous technical uses, simplicity in manufacture, low eddy current barriers, and adjustable properties. (Khan et al., 2021). Ferrite is the material most frequently connected with the nanotechnology revolution. In addition, ferrite nanoparticles display qualities like surface heterogeneity and super paramagnetism and have a high surface-to-volume ratio compared to materials used in whole parts. (Taneja et el., 2021). The production of ferrites nanoparticles may be influenced by a number of variables, including calcination duration and temperatures, early solution pH, fuel to oxidizer ratio, combustion assistance, and others. (Shayestefar et al., 2021). Understanding how dopants alter the magnetism of m-type spinel ferrites is the main objective of this study. To that purpose, we shall discuss the concept of ferrite, its varieties, and the low-cost, environmentally-friendly "sol-gel" process of synthesis.

2. Hexaferrite

Hexaferrite is a subclass of ferrite that has seen a marked increase in scientific research; as such, this material is significant both competitively and technically, being responsible for the majority of magnetic materials designed and manufactured globally. In 1952, the material was noticed in a Philips laboratory. H. P. J. Wijn and J. Smit spent a long time debating its properties. The unit cell of the crystal is typically understood by ($a = b \approx 5.90$ and, $c \approx 23.30$), as well as the ceramic object's relevant space group is P63/mmc. (Trukhanov et al., 2018). This hexagonal structure has a distinct c-axis and is significantly more complex than spinel and other ferrites. As a result, adjusting the magnetization direction to another axis is difficult (Pullar, 2012). As permanent magnets, hexagonal ferrites have indeed been widely used. Since of their low cost and richness of raw goods, they are structurally and chemically stable, have high coercivity, and are resistant to corrosion. (Rhein et al., 2018), (Trukhanov et al., 2018). These properties make it a prospective alternative for overpriced permanent magnets such as rare earth alloys and relevant in diverse areas such as magnetic refrigeration, wireless communication, high-frequency devices up to many gigahertz (Bai

et al., 2015), ferrofluids, and perpendicular recording (Khan et al., 2021).

Three basic blocks are stacked together to form hexaferrite structures. Hexagonal ferrites can be classified based on their chemical formulas and crystal structure into M, X, Y, W, U, R, and Z-type hexagonal ferrites (Bai et al., 2015), (Akhter et al., 2022), (Ejaz et al., 2018). The spread of iron ions inside this crystallographic lattice determines the ionic conductivity of hexaferrite (Chavan et al., 2016). Numerous studies, on the other hand, have concentrated on substituted hexaferrite, in which certain iron cations are changed by other elements (e.g. In, Sc, Ga, Ti.). However, many studies have focused on substituted hexaferrite, where such iron cations are changed by other elements (e.g. In, Sc, Ga, Ti.). This modification alters the processability of hexaferrite, such as its magnetic and radio-absorbing properties, and widens options for improving established ferrite devices or inspiring the development of fresh ones (V.G. et al., 2022). Hexaferrite, a multiferroic with combined electric and magnetic polarizations and greater magnetoelectric coupling, was recently discovered (Aghazadeh et al., 2017), (Martínez-Pérez et al., 2019)

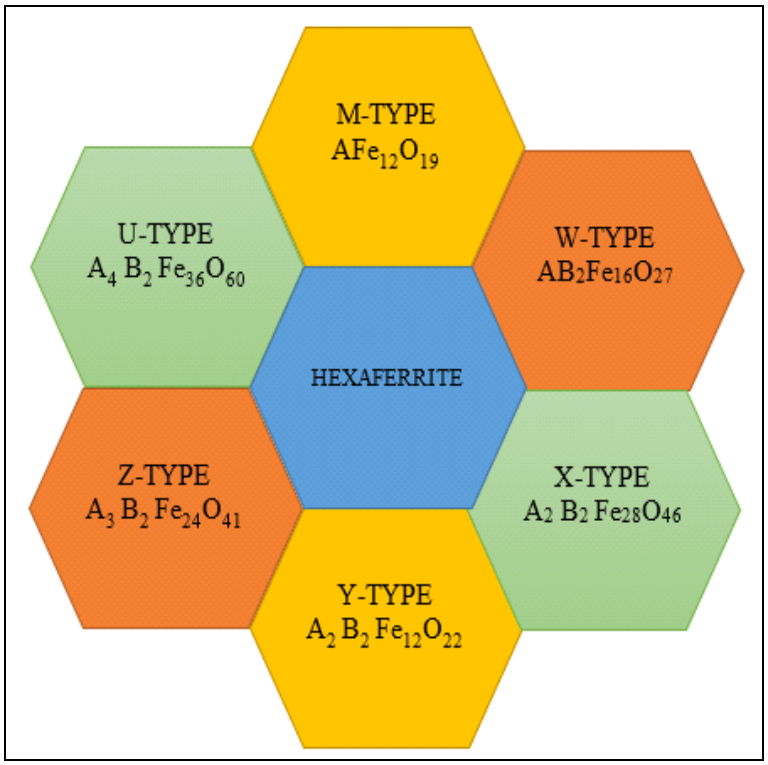

Figure 1. Illustration of the Hexaferrite classification

2.1. Hexaferrite M-type

M-type hexaferrite is one of the most amazing or extensively studied permanent magnetic resources among ferrimagnetic oxides. The influence of such ferrite nanoparticles on technological breakthroughs has been intensively studied since the time of the M-type ferrite breakthrough in Philips labs in the Holland in the 1950s (Hazra and Ghosh, 2014). The M-type hexaferrite has excellent chemical hardness and corrosion resistance, as well as low production costs, greater electrical resistance, a large dielectric, and low magnetic loss (Patel et al., 2020). Additionally, saturation magnetization, high permeability, and magneto-crystalline anisotropy are all characteristics of M-type hexaferrite. Grain boundary translation and magnetism (spin) rotation are the two mechanisms in charge of regulating the permeable of this substance. Due to the significant magneto-crystalline anisotropy of hexaferrite, magnetization rotations is the more important of the two mechanisms. At lower applied frequencies, the

domain wall movement becomes more pronounced. The magnetic material's complicated permeability is prompted by magnetization (spin) rotation, which exists when the magnetic anisotropy of the hexaferrite increases with frequency. As soon as the transmitted field is modified, the grain boundary shift and rotations of the material's magnetism are detected (Mathews and Babu, 2021), along with the loss of the magnetic component (") that follows (Mathews and Babu, 2021). A high-density deposit made of iron, oxygen, and barium ions crystallizes at interstitial locations to form Ca, Ba, and Sr-based M-type hexaferrites. Blocks with the letters S (spinal) and R (hexagonal) make up the crystal structure. The S block, which is a two-layered oxygen shape with the chemical formula $Fe_6O_8^+$ and the R block, which is a three-layered oxygen shape with the chemical formula $Sr/BrFe_6O_{11}^{2-}$, are stacked on top of one another and follow the sequence SRS*R* along the crystallographic axis (c-axis) to form SrM/BaM, where * denotes that the S and R blocks rotate

Figure 3 depicts the five crystallographic locations where the Fe^{3+} ion may be found in the structure (Rana et al. 2016), (Bai et al., 2000). Because ferrites coupling initiates the super-exchanged state, $Fe^{3+} - O^{2-} - Fe^{3+}$ interactions and the space about them bonds (Rana et al. 2016), the atomic magnetic sequences of the five Fe^{3+} sub-lattices change direction, the spin directions of the different magnetic brief seconds of these Fe^{3+} ions were indeed attributed to antagonistic effects. Additionally, at places 2a, 2b, and 2k, Fe^{3+} ions increase the net magnetic moment, whereas 4f1 and 4f2 sites decrease it (Xu et al., 1990). Therefore, the intrinsic magnetism can be enhanced by replacing the Fe^{3+} particles in various crystallographic positions with other suitable ions. As a result, the following equation may be used to determine the accumulated magnetic properties in M-type hexaferrite:

$$M_{TOTAL}(T) = [6M_{12k}(T) + 1M_{2b}(T) + 1M_{2a}(T)] \uparrow - [2M_{4f1}(T) + 2M_{4f2}(T)] \downarrow \quad (1)$$

Where Mn describes the magnetic moment of Fe^{3+} ion in the nth sublattice.

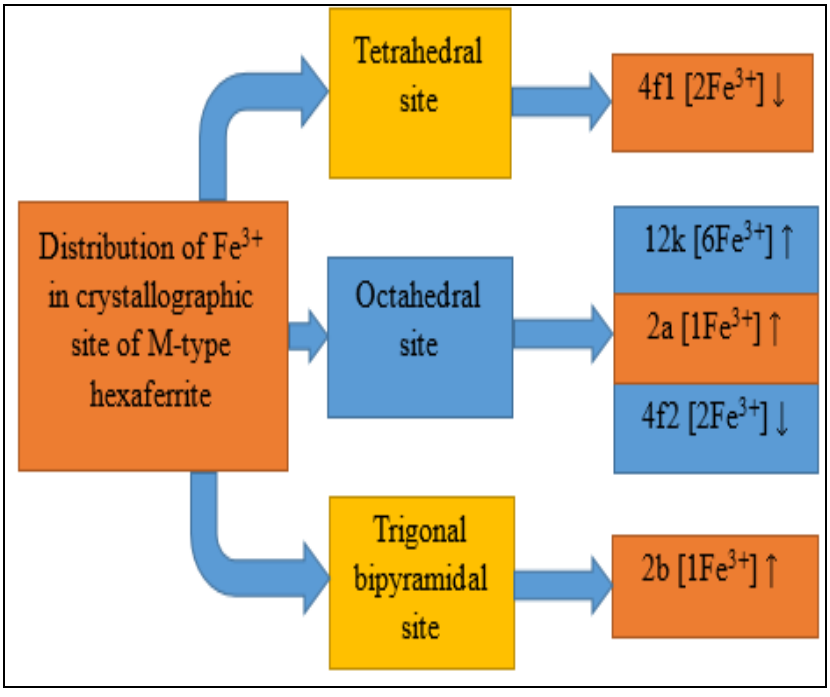

Figure 2. Sketch of distribution of Fe^{3+} on five interstitial sites of M-type hexaferrite

Fridge door magnets, microwave devices, magnetic recording devices, transformers, magnetic hoses, super - capacitors, loudspeaker magnets, and electromagnetic shielding devices all use M-type ferrite materials (Tchouank Tekou Carol et al., 2017), (Sharma et al., 2017). High electrical

resistivity materials with low dielectric permittivity, dissipation factor, and drift movement value are best suited for use with a dielectric filler in microwave appliances and electromagnetic damping (Roohani et al., 2017). Furthermore, in recording media tools, materials with minimal coercivity and greater saturation magnetization values are required (Davoodi & Hashemi, 2011)

3. Review on effect of dopant on magnetic properties

A vibrating specimen magnetometer was used to assess the characteristics of ferrite (VSM). According to the vast majority of research, synthesis circumstances, composition, and sintering all significantly affect characteristics (Khan et al., 2017). The distribution of metal ions over the tetrahedral and octahedral surfaces also significantly affected the characteristics of ferrites (Ghazi et al., 2018). Han et al. (2021) fabrication of a composite with the formula $BaFe_{12-x}Al_xO_{19}$ (x = 0, 1, 2, 4, 6) revealed from magnetic characteristics that Al^{3+} concentration and temperature had a considerable impact on coercivity. $BaFe_8Al_4O_{19}$ reached the maximal coercivity of $H_C = 13.7KOe$, which is an improvement of 1.686 above $BaFe_{12}O_{19}$. M-type hexaferrite doped with various concentrations of Pr has been created by (Abbas et al. 2015). With the exception of the specimen with x=0.10 concentrations, which demonstrates distinct outcomes, the investigation clarified the harsh magnetism performance of all specimens. Strong Ms and low Hc therefore improve sample penetration, which is advantageous for microwave devices. Investigations into the impact of Al-Mn substitution on the magnetic characteristics of M-type magnesium hexagonal ferrites nanoparticles show that magnetic parameters like Hc, Mr, and Ms rise with Al-Mn concentration (Mohammed et al. 2019). When x=0.2, the coercivity, Hc = 4597.58 Oe, was noticed. Applications using high-frequency might make advantage of the material. Sm-doped strontium ferrite nanopowders $(SrSm_{0.3}Fe_{11.7}O_{19})$ and polyaniline (PANI)/Sm-doped cesium ferrite nanocomposite with 10 weight percent and 20 weight percent ferrites are scrutinized by (Luo et al., 2014), in their study published. With a paring thickness of three millimeters, the ferromagnetic composite had the greatest absorption performance in the spectrum area of $2 \times 10^{18} GHz$.

In a report on the synthesis of hexaferrite with the formula $Sr_{1-x}Nd_xFe_{11-x}Co_xO_{19}$ by (Herme et al., 2012), at x=0.2, Hc increases by 0.11 to 68.9 A/m (5480 Oe), while Ms decreases by 0.06 to $(91Am^2/kg)$. Slimani et al. (2018) create a nanospinel ferrites composite $(Li_{2x}Cu_{1-x}Al_yFe_{2-y}O_4)$ using the hydrothermal method. When Li and Al were present in the mixture at different concentrations, the anisotropy constant was improved at (x, y =0.2), but decreased when the doping content increased. Meanwhile, the result showed a squareness ratio of less than 0.50 for (x, y=0.4), indicating that the nanoparticles are single domain with uniaxial anisotropy for (Li). Khan et al., (2021) investigates properties of $Sr_2Cu_xNi_{2-x}Cr_xFe_{28-x}O_{46}$ (x = 0.0, 0.1, 0.2, 0.3, 0.4, 0.5). It was discovered that pure X-type ferrites exist. The incorporation of cations caused significant variations in Hc, Ms, and Mr. The report suggested that these materials can be used in longitudinal recording media. Gupta et al., (2020) made a set of Erbium substituted X-type hexaferrite composite $Ba_2Co_2Er_xFe_{28-x}O_{46}$ (x = 0.00, 0.04, 0.08, 0.12, 0.16, and 0.20). For x = 0.12, the subsequent result were presented, $M_S = 52.29Am^2/kg$ and $H_a = 1370KA/m.$ Shezad et al., (2020) investigate the properties of $SrY_xFe_{12-2x}Ni_xO_{19}$ (SrYFeNiO). Magnetic parameters were reduced by the addition of Y^{3+} and $Ni^{3+}.I$n addition, for x = 0.15, the coercivity $H_C = 2.92KOe$ and anisotropy $K = 5.79 \times 10^6 Erg/g$ were shown. Thus, the ceramic is suitable for use in the permanent magnetic industry.

4. Synthesis of Hexaferrite

The most common method of synthesizing M-type hexagonal ferrites is depicted in Diagram 2. A solution combustion approach is used in the sol-gel method (Sutka & Mezinskis, 2012). Reduced heating temperature, improved homogeneity, better particle size and ultrafine particles, morphology control, short processing time, high purity of the finished product, and low external energy demand are just a few of the advantages of this technique (Patel et al., 2020). The sol-gel sequence starts with disintegrating metal nitrates in the preferred solvent, accompanied by a constant stirring of the solution. A chelating agent solution is typically added to the above solution to allow for the formation of complex structures. By adding ammonia solution drop by drop, the pH of the solution is kept stable. Gel formation occurs later as a result of heating. This gel is annealed at a specific temperature to produce the desired material (Kumar et al., 2017).). In the sol-gel auto combustion method, the fuel serves as a combustion, complexing, chelating, capping, and reducing agent. PVA (Chawla et al., 2015), surfactant (N-decyl-trimethylammonium bromide (Martínez-Pérez et al., 2019), green fuel (sucrose, fructose, maltose), or natural fuel (Aloe Vera extract, cherry juice, and neem leaves extract (Godara et al., 2021). The magnetic, dielectric, surface morphology, grain shape, and calcination temperature of hexaferrite are determined by the fuel type.

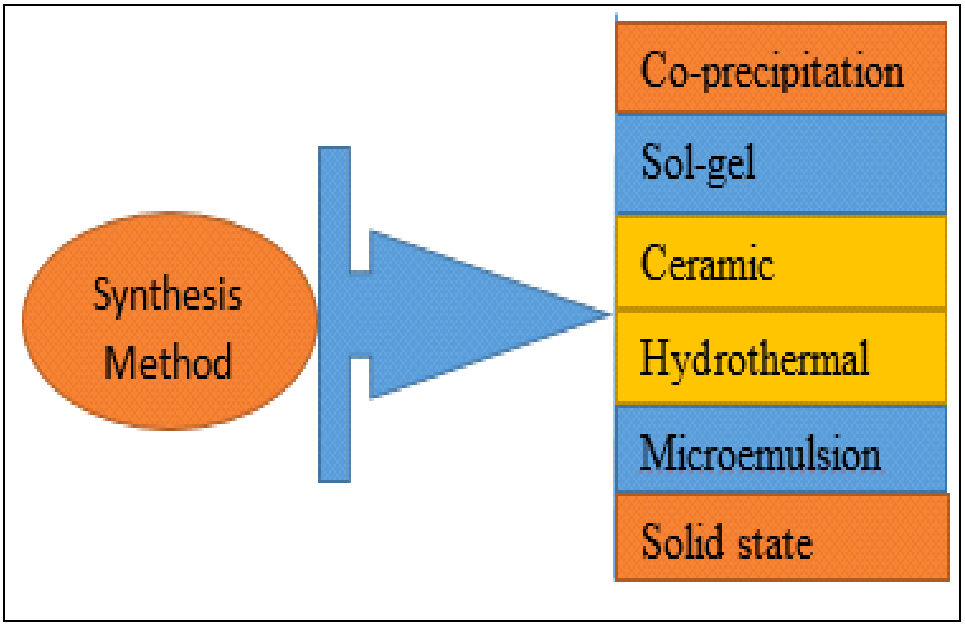

Figure 3. Method of Synthesis of Hexaferrite

4.1 Sol-gel synthesis of doped Hexaferrite

In order to make strontium ferrite nanoparticles, the sol-gel method was utilized. Strontium nitrate anhydrous granule, iron (III) nitrate, A-nitrate (A is a dopant element), citric acid, ammonium, and deionized were employed as the procedure's raw materials. Strontium nitrate and iron (III) nitrate are dissolved in 100 milliliters of water for many minutes at 60 degrees Celsius with a steady stirrer rotation of 250 rpm to create aqueous solutions. The temperature was increased to 80 °C, and citric acid were added as a coagulant at a citric to nitrate molarity of 0.75 (C/N = 0.75). Ammonia was introduced to the mixes, which were vigorously stirred, to change the pH from 0 to 8. The pH was measured using a pH meter. After a few hours of stirring and heating at 90 °C, the solution was effectively transformed into a green sticky gel. After forming a thick, gooey gel, the heater's temperatures are raised to 200 degrees Celsius, and the gels are burned for an hour to finish the dehydrating process. The powder samples

underwent a 6-hour heat treatment at 900 °C (Azis et al., 2018)

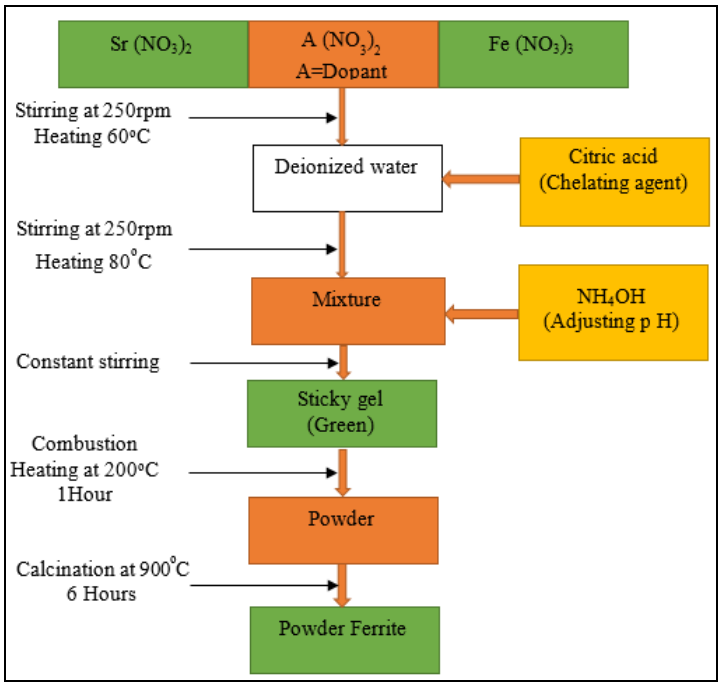

Figure 4. Schematic representation of the sol–gel process of A-doped Hexaferrite

5. Determination of Magnetic Properties

Utilizing a magnetometer to create the polarization (hysteresis) curves is the most well-known method of evaluating the magnetization in ferrite (Nisticò et al., 2020). By varying the externally applied field, the test specimen is applied to a magnetic moment closed loop in an oscillating sample magneto (VSM). It is intended for the magnetization of the substance to be a nonlinear function that symbolizes the concentration of magnetic moments. The measurement result is then communicated via a loop. In actuality, the field in which ferrites are used depends on the geometry of the magnetic transition region. The circles with the subsequent parameters—coercivity, magneto crystalline anisotropy constant, remanence magnetization, squareness ratio, and saturation magnetization—showcase the ferrite ceramic.

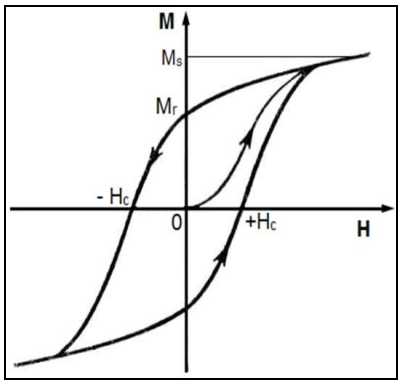

Figure 5. Magnetization curve (Hysteresis) for ferrite

5.1 Saturation magnetization Ms, denotes the greatest field that a material can produce. It is influenced by the density and reliability of the dipole moments just on atoms that comprise the material.

5.2 The Squareness ratio: the squareness ratio of a ferrite sample is an assessment of how comparable the material is to being optimistic. The ferrite material's loop could be square or non-square. A perfect hard magnet has a square hysteresis loop. It can be calculated using formula:

$$Squareness\ ratio = \frac{M_r}{M_s}$$

According to scientific findings, magnetic materials with a squareness ratio of greater or equal to 0.5 are said to have a single magnetic domain (Naeem Ashiq et al., 2017). In addition materials with a squareness ratio of less than or equal to 0.5 are thought to have multiple magnetic domains (Batool et al., 2022).

5.3 Remanence magnetization and Coercivity

Remanence (Mr) is the magnetism left in a material once the magnetizing field has been distant. While coercivity (Hc) measures how much magnetic intensity is needed to demagnetize a magnet. The coercivity (Hc) of non-interacting magnetic nanoparticles in a single domain is granted by the equation.

$$H_C = \frac{K^4 D^6}{M_S A^8} \quad (3)$$

5.4 Crystalline magneto anisotropy

The amount of energy necessary to distract the magnetic moment in a single crystal from a simple to a tough direction is referred to as magnetocrystalline anisotropy. The connection of the spin magnetic moment with the crystal lattice (spin-orbit coupling) is responsible for the easy and difficult directions. (Su et al., 2022). The demagnetization process in hexagonal ferrites with a single domain structure is the rotation of the domain magnetic moment, and the main factor influencing domain rotation is the magnetocrystalline anisotropic energy. The crystalline magneto anisotropy is calculated by using equation (Gan et al., 2018)

$$K = \frac{M_S \cdot H_C}{0.96} \quad (4)$$

This equation shows that the Hc is proportional to the anisotropy constant and inversely proportional to the Ms, which explains why, as the anisotropy constant increases or decreases, the whole samples may have a little higher or lower coercivity.

The Bohr magneton number or magnetic moment of synthesized ferrite samples is defined by the formulas (Potangale & Pardeshi, 2022)

$$\mu_B = \frac{M_W \cdot M_S}{5585} \quad (5)$$

6. Result and discussion

The magnetic parameters of the prepared sample are expressed in Table 1. The Squareness ratio of the first three samples is less than 0.5, indicating that the nanoparticle contains multiple magnetic domains, whereas when the dopant concentration is x=1.0, the material prepared has a single magnetic domain (Yassine et al., 2022). Explains that for a squareness value just under 0.5, magnetostatic interaction between them is possible, while for a squareness value greater than 0.5, particle sharing is irregular and non-interacting. As a consequence, the particles are interacting magnetostatically, and this is how a magnetic particle interacts with its neighbor, giving rise to the magnetic properties of the entire material. This demonstrated that the Squareness ratio is directly related to saturation and remanence magnetization. The lowest and highest coercivity of the measurement are 663.245 and 1633.636Oe.

Table 4. The VSM result of $Ba_{1-x}Ca_xFe_{11.4}Al_{0.6}O_{19}$ (Yousaf et al., 2021)

Samples	Ms(emu/g)	Mr(emu/g)	Mr/Ms	Hc(Oe)	K
X=0.00	46.652	22.531	0.4829	663.245	32230.94
X=0.33	48.631	18.724	0.3850	1030.371	52195.80
X=0.66	50.363	21.842	0.4336	1528.517	80188.23
X=1.00	47.085	23.745	0.5043	1633.636	80124.76

Figure 2 depicts the hysteresis loops of $Ba_{1-x}Ca_xFe_{11.4}Al_{0.6}O_{19}$ at various calcium concentrations. The loop has the same shape, but the interception along the vertical and horizontal axes occurs at a different point due to dopant variation. Along the perpendicular axis, the peak remanence magnetization is 23.745 emu/g, which occurs when x=1.0, and the lowest value is 18.724 emu/g, which occurs when 0.33 percent calcium is introduced. According to the graph, the minimum saturation magnetization occurs when the material is pure, but when the dopant is present, the values increase.

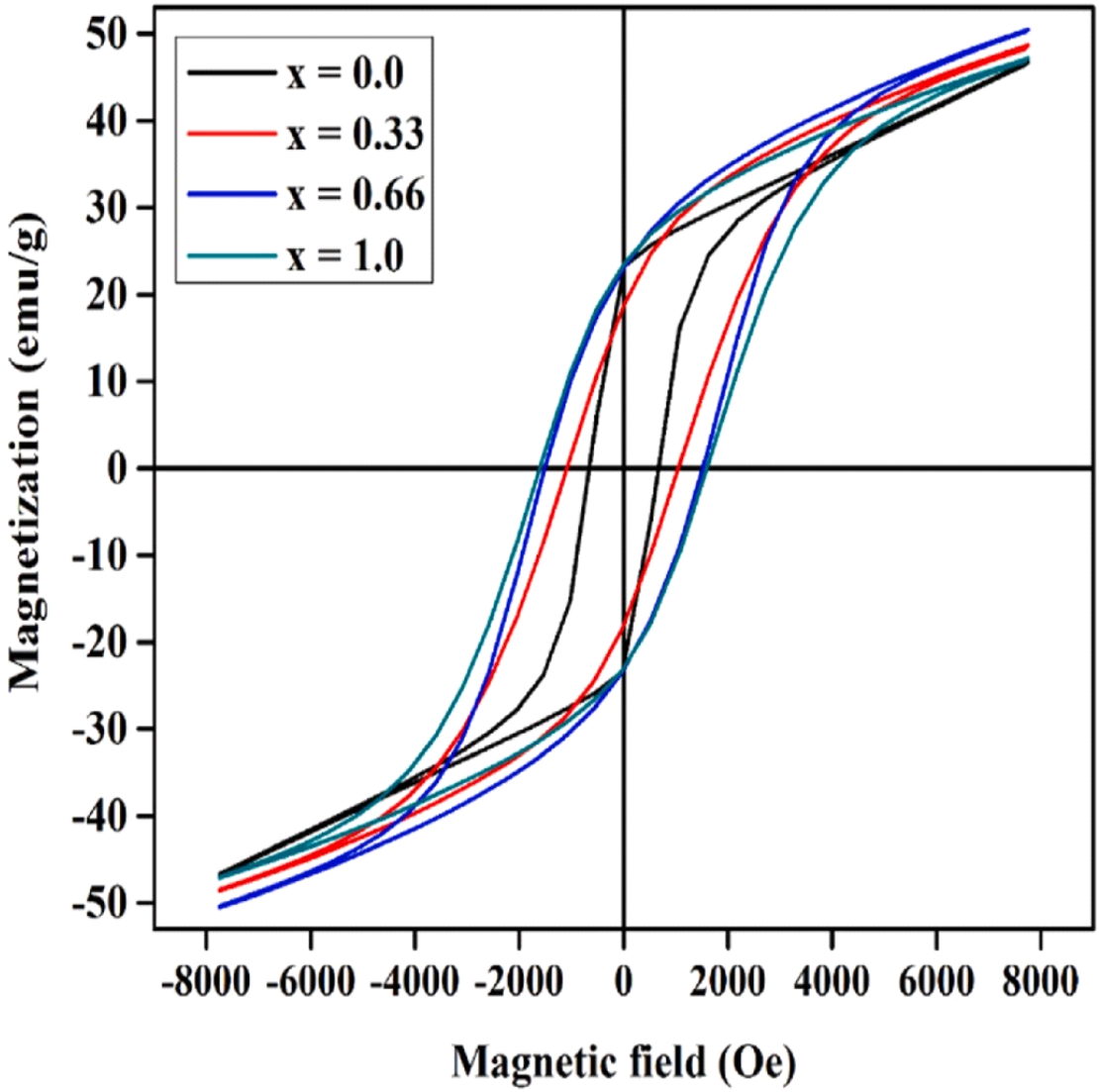

Figure 6. The display of M versus H loop of $Ba_{1-x}Ca_xFe_{11.4}Al_{0.6}O_{19}$ (Yousaf et al., 2021)

The remanence and saturated magnetization values for the sample were extracted directly from figure 2 the remanence magnetization values decrease when aluminium is substituted in the ferrite. The decrease is caused by the parent material's changeover of non-magnetic ions for iron ions. Remember that Fe ions are distributed among the five crystallographic sides of ferromagnetic materials and have different spin directions. As a result, if the Fe^{3+} ions are swapped at spin-up sites, Ms will decrease while increasing at spin-down sites. Thus, replacing Fe^{3+} with Al^{3+} reduces the unpaired spin magnetic moment, requiring less energy (from the external magnetic field) to direct the spin, as evidenced by a reduction in saturation magnetization from 68 to 30 emu/g, resulting in decreased susceptibility (Xm)

and permeability (r). In the case of coercivity H_c, its values range from 479 to 8249 Oe as x values vary (Rai et al., 2013) According to the literature, the hexaferrite nanoparticle has sizes less than 1m for a high value of coercivity and is claimed to be a non-interacting uniaxial, single domain, and disorganized nanoparticle. (Pereira et al., 2009), hard magnetic materials have a coercivity of about 3.77KOe, so the examples in this work met the theory.

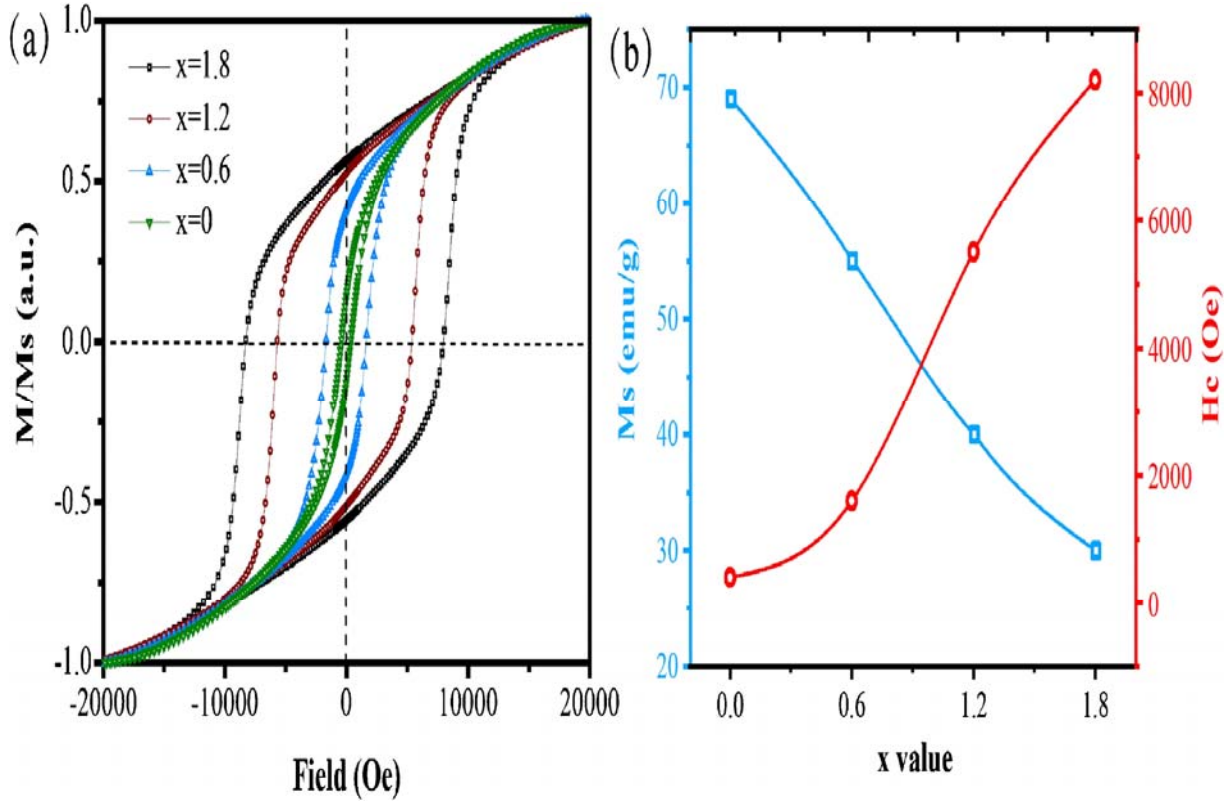

Figure 7. (a) Hysteresis loops of $BaFe_{12-x}Al_xO_{19}$ at varied Al ion concentration (Zhou et al., 2021)

7. Conclusion

Many permanent magnet resources have been discovered in the last century. Strategies for successfully producing these magnets have been demonstrated. Device configurations incorporating such magnets have been usefully exploited in a wide range of active and passive uses. Permanent magnets are the best choice for many uses as they provide a consistent field without the ongoing costs of electricity or heat generation. This paper provided an overview of the magnetic performance of m-type hexaferrite with various dopants. There was also information about the classification of m-type hexaferrite. The method of sol-gel synthesis for m-type hexaferrite was described. The iron ion crystallographic site was highlighted. According to hysteresis loop analysis, the setting of non-magnetic or less magnetic ions in the 4f1 and 2b polyhedral sites of iron ions resulted in a decrease in magnetic factors such as saturation magnetization (Ms) and remnant magnetization.

References

1. Abbas, W. (2015) "Structural and magnetic behavior of Pr-substituted M-type hexagonal ferrites synthesized by sol-gel autocombustion for a variety of applications," J. Magn. Magn. Mater., vol. 374, pp. 187–191, doi: 10.1016/j.jmmm.2014.08.029.
2. Aghazadeh, M., Karimzadeh, I., & Ganjali, M. R. (2017). Ethylenediaminetetraacetic acid capped superparamagnetic iron oxide (Fe3O4) nanoparticles: A novel preparation method

and characterization. Journal of Magnetism and Magnetic Materials, 439, 312–319. https://doi.org/10.1016/j.jmmm.2017.05.042

3. Akhter, T., Khan, H. M., Honey, S., Hussain, S. S., Zahid, M., Javed, M. S., Alshgari, R. A., Mushab, M. S. S., Bocchetta, P., & Ansari, M. Z. (2022). Optimization of structural, electrical, and magnetic properties of ytterbium substituted W-type hexaferrite for multi-layer chip inductors. Ceramics International, April. https://doi.org/10.1016/j.ceramint.2022.07.258
4. Almessiere, M. A., (2021). Electronic, magnetic, and microwave properties of hard/soft nanocomposites based on hexaferrite SrNi0.02Zr0.02Fe11.96O19 with variable spinel phase MFe2O4 (M = Mn, Co, Cu, and Zn), Ceram. Int., vol. 47, no. 24, pp. 35209–35223, , doi: 10.1016/j.ceramint.2021.09.064.
5. Almessiere, M. A., (2021). Sm–Dy co-substituted Sr hexaferrite microspheres: An investigation on their structural, magnetic, optical, and porosity characteristics, Ceram. Int., vol. 47, no. 17, pp. 25131–25141, doi: 10.1016/j.ceramint.2021.05.243.
6. Auwal, I. A., Güngüneş, H., Baykal, A., Güner, S. Shirsath, S. E., and Sertkol, M.(2016). Structural, morphological, optical, cation distribution and Mössbauer analysis of Bi3+ substituted strontium hexaferrite, Ceram. Int., vol. 42, no. 7, pp. 8627–8635, doi: 10.1016/j.ceramint.2016.02.094.
7. Bai, J., Liu, X., Xie, T., Wei, F., and Yang, Z. (2000). Effects of La-Zn substitution on the magnetic properties of Sr-magnetoplumbite ferrite nano-particles, Mater. Sci. Eng. B Solid-State Mater. Adv. Technol., vol. 68, no. 3, pp. 182–185, doi: 10.1016/S0921-5107(99)00593-0.
8. Bai, Y., Zhang, W., Qiao, L., & Cao, J. (2015). Engineering soft magnetic properties by doping ions in low-fired M-type hexaferrite with Bi-Co-Ti substitution. RSC Advances, 5(111), 91382–91388. https://doi.org/10.1039/c5ra17542a
9. Batool, S. R., Malana, M. A., Alfryyan, N., Ashiq, M. N., Aftab, F., Aman, S., Khan, S. A., Alrowaili, Z. A., Al-Buriahi, M. S., & Alomairy, S. (2022). Synthesis, characterization, dielectric and magnetic properties of substituted Y-type hexaferrites. Journal of Materials Science: Materials in Electronics, 33(20), 16183–16196. https://doi.org/10.1007/s10854-022-08508-y
10. Chavan, V. C., Shirsath, S. E., Mane, M. L., Kadam, R. H., & More, S. S. (2016). Transformation of hexagonal to mixed spinel crystal structure and magnetic properties of Co2+ substituted BaFe12O19. Journal of Magnetism and Magnetic Materials, 398, 32–37. https://doi.org/10.1016/j.jmmm.2015.09.002
11. Chawla, S. K., Kaur, P., Mudsainiyan, R. K., Meena, S. S., & Yusuf, S. M. (2015). Effect of Fuel on the Synthesis, Structural, and Magnetic Properties of M-Type Hexagonal SrFe12O19 Nanoparticles. Journal of Superconductivity and Novel Magnetism, 28(5), 1589–1599. https://doi.org/10.1007/s10948-014-2893-5
12. Godara, S. K. (2020). Synthesis and characterization of Jamun pulp based M-type barium hexaferrite via sol–gel auto-combustion, Results Phys., vol. 22, p. 103903, 2021, doi: 10.1016/j.rinp.2021.103903.
13. Davoodi, A., & Hashemi, B. (2011). Magnetic properties of Sn-Mg substituted strontium hexaferrite nanoparticles synthesized via coprecipitation method. Journal of Alloys and Compounds, 509(19), 5893–5896. https://doi.org/10.1016/j.jallcom.2011.03.002
14. Ejaz, S. R., Khan, M. A., Warsi, M. F., Akhtar, M. N., & Hussain, A. (2018). Study of structural transformation and hysteresis behavior of Mg-Sr substituted X-type hexaferrites. Ceramics International, 44(15), 18903–18912. https://doi.org/10.1016/j.ceramint.2018.07.126

15. Gan, G., Zhang, H., Li, Q., Li, J., Huang, X., Xie, F., Xu, F., Zhang, Q., Li, M., Liang, T., & Wang, G. (2018). Low loss, enhanced magneto-dielectric properties of Bi2O3 doped Mg-Cd ferrites for high frequency antennas. Journal of Alloys and Compounds, 735, 2634–2639. https://doi.org/10.1016/j.jallcom.2017.12.002
16. Ghazi, N., Mahmoudi Chenari, H., and Ghodsi, F. E. (2018). Rietveld refinement, morphology analysis, optical and magnetic properties of magnesium-zinc ferrite nanofibers, J. Magn. Magn. Mater., vol. 468, pp. 132–140, doi: 10.1016/j.jmmm.2018.07.084.
17. Godara, S. K., Dhaka, R. K., Kaur, N., Malhi, P. S., Kaur, V., Sood, A. K., Bahel, S., Bhadu, G. R., Chaudhari, J. C., Pushkarna, I., & Singh, M. (2021). Synthesis and characterization of Jamun pulp based M-type barium hexaferrite via sol–gel auto-combustion. Results in Physics, 22(October 2020), 103903. https://doi.org/10.1016/j.rinp.2021.103903
18. Gupta, T., Chauhan, C. C., Kagdi, A. R., Meena, S. S., Jotania, R. B., Singh, C., & Basak, C. B. (2020). Investigation on structural, hysteresis, Mössbauer properties and electrical parameters of lightly Erbium substituted X-type Ba2Co2ErxFe28-xO46 hexaferrites. Ceramics International, 46(6), 8209–8226. https://doi.org/10.1016/j.ceramint.2019.12.049
19. Han, G. (2020). Structure and magnetic properties of the porous Al-substituted barium hexaferrites, J. Magn. Magn. Mater., vol. 528, pp. 1–7, 2021, doi: 10.1016/j.jmmm.2021.167824.
20. Harrison, R. J., Dunin-Borkowski, R. E., and Putnis, A. (2002). Direct imaging of nanoscale magnetic interactions in minerals, Proc. Natl. Acad. Sci. U. S. A., vol. 99, no. 26, pp. 16556–16561, doi: 10.1073/pnas.262514499.
21. Hazra, S. and Ghosh, N. N. (2014). Preparation of nanoferrites and their applications, J. Nanosci. Nanotechnol., vol. 14, no. 2, pp. 1983–2000, doi: 10.1166/jnn.2014.8745.
22. Herme, C. A., Bercoff, P. G., & Jacobo, S. E. (2012). Nd-Co substituted strontium hexaferrite powders with enhanced coercivity. Materials Research Bulletin, 47(11), 3881–3887. https://doi.org/10.1016/j.materresbull.2012.08.047
23. Kaur, A. and Bhargava, G. K. (2020). Review paper on nickel-zinc nano ferrite, Mater. Today Proc., vol. 37, no. Part 2, pp. 3082–3086, doi: 10.1016/j.matpr.2020.09.016.
24. Kesavan, G., Pichumani, M., Chen, S. M., & Ko, C. S. (2022). Surfactant-assisted (CTAB, PVA, PVP) thermal decomposition synthesis of strontium spinel ferrite nanocrystals for electrochemical sensing of cytostatic drug flutamide. Materials Today Chemistry, 26. https://doi.org/10.1016/j.mtchem.2022.101045
25. Khan, M. A., Qamar uz Zaman, M., Majeed, A., Akhtar, M. N., & Abbas, W. (2021). Structural, spectral, dielectric and magnetic properties of Sr2CuxNi2-xFe28-xCrxO46 ($0 \leq x \geq 0.5$) ferrites synthesized via micro-emulsion route. Materials Chemistry and Physics, 259(November 2020), 124066. https://doi.org/10.1016/j.matchemphys.2020.124066
26. Khan, M. A. (2017). Structural, magnetic and dielectric properties of Yb3+doped BaCo-X hexagonal nanoferrites, J. Alloys Compd., vol. 695, pp. 3674–3681, doi: 10.1016/j.jallcom.2016.11.369.
27. Kumar, A., Kumar, V., & Ghumman, S. S. (2017). Synthesis and characterization of titanium doped barium ferrite and effects of doping on electrical and magnetic properties of the compound. Ferroelectrics, 519(1), 82–89.

https://doi.org/10.1080/00150193.2017.1361215

28. Luo, J., Xu, Y., and Gao, D. (2014). Synthesis, characterization, and microwave absorption properties of polyaniline/Sm-doped strontium ferrite nanocomposite, Solid State Sci., vol. 37, pp. 40–46, doi: 10.1016/j.solidstatesciences.2014.08.007.
29. Martínez-Pérez, J. P., Bolarín-Miró, A. M., Pedro-García, F., Cortés-Escobedo, C. A., Barba-Pingarrón, A., & Sánchez-De Jesús, F. (2019). Magnetic and dielectric characterization of xBiFeO3:(1-x)SrFe12O19 multiferroic composites. Journal of Alloys and Compounds, 808, 3–10. https://doi.org/10.1016/j.jallcom.2019.151700
30. Mathews, S. A. and Babu, D. R. (2021). Analysis of the role of M-type hexaferrite-based materials in electromagnetic interference shielding, Curr. Appl. Phys., vol. 29, no. June, pp. 39–53, doi: 10.1016/j.cap.2021.06.001.
31. Mohammed, J. (2019). Structural, dielectric and magnetic properties of Al-Mn substituted nano-sized M-type strontium hexagonal ferrites," Mater. Today Proc., vol. 18, pp. 533–541, , doi: 10.1016/j.matpr.2019.06.392.
32. Naeem Ashiq, M., Sami Asi, A., Farooq, S., Najam-ul-Haq, M., & Rehman, S. (2017). Magnetic and electrical properties of M-type nano-strontium hexaferrite prepared by sol-gel combustion method. Journal of Magnetism and Magnetic Materials, 444, 426–431. https://doi.org/10.1016/j.jmmm.2017.08.065
33. Patel, C. D., Dhruv, P. N., Meena, S. S., Singh, C., Kavita, S., Ellouze, M., & Jotania, R. B. (2020). Influence of Co4+-Ca2+ substitution on structural, microstructure, magnetic, electrical and impedance characteristics of M-type barium–strontium hexagonal ferrites. Ceramics International, 46(16), 24816–24830. https://doi.org/10.1016/j.ceramint.2020.05.326
34. Pereira, F. M. M., Santos, M. R. P., Sohn, R. S. T. M., Almeida, J. S., Medeiros, A. M. L., Costa, M. M., & Sombra, A. S. B. (2009). Magnetic and dielectric properties of the M-type barium strontium hexaferrite (Ba xSr1-xFe 12 O 19) in the RF and microwave (MW) frequency range. Journal of Materials Science: Materials in Electronics, 20(5), 408–417. https://doi.org/10.1007/s10854-008-9744-8
35. Potangale, C. N., & Pardeshi, S. K. (2022). Effect of Ni2+ substitution on magnetic, optical and electrical properties of SrFe2O4. Materials Science and Engineering B: Solid-State Materials for Advanced Technology, 283(July 2021), 115848. https://doi.org/10.1016/j.mseb.2022.115848
36. Pullar, R. C. (2012). Hexagonal ferrites: A review of the synthesis, properties and applications of hexaferrite ceramics. Progress in Materials Science, 57(7), 1191–1334. https://doi.org/10.1016/j.pmatsci.2012.04.001
37. Rana K. (2016). Influence of samarium doping on magnetic and structural properties of M type Ba-Co hexaferrite, Ceram. Int., vol. 42, no. 7, pp. 8413–8418, 2016, doi: 10.1016/j.ceramint.2016.02.058.
38. Rai, B. K., Mishra, S. R., Nguyen, V. V., & Liu, J. P. (2013). Synthesis and characterization of high coercivity rare-earth ion doped Sr0.9RE0.1Fe10Al2O19 (RE: Y, La, Ce, Pr, Nd, Sm, and Gd). Journal of Alloys and Compounds, 550, 198–203. https://doi.org/10.1016/j.jallcom.2012.09.021
39. Rhein, F., Helbig, T., Neu, V., Krispin, M., & Gutfleisch, O. (2018). In-situ magnetic force microscopy analysis of magnetization and demagnetization behavior in Al3+ substituted Sr-hexaferrite. Acta Materialia, 146, 85–96. https://doi.org/10.1016/j.actamat.2017.12.010
40. Roohani, E., Arabi, H., Sarhaddi, R., & Sudkhah, S. (2017). M-Type Strontium Hexaferrite Nanoparticles Prepared by Sol-Gel Auto-combustion Method: The Role of Co Substitution in Structural, Morphological,

and Magnetic Properties. Journal of Superconductivity and Novel Magnetism, 30(6), 1599–1608. https://doi.org/10.1007/s10948-016-3966-4

41. Sharma, J., Kumar, A., Kumar, S., & Srivastava, A. K. (2017). Investigation of structural and magnetic properties of Tb–Ni-doped bismuth ferrite nanoparticles by auto-combustion method. Applied Physics A: Materials Science and Processing, 123(8). https://doi.org/10.1007/s00339-017-1140-x
42. Shayestefar, M., Mashreghi, A., Hasani, S., and Taghi Rezvan, M. (2021). Optimization of the structural and magnetic properties of MnFe2O4 doped by Zn and Dy using Taguchi method, J. Magn. Magn. Mater., vol. 541, no. p. 168390, 2022, doi: 10.1016/j.jmmm.2021.168390.
43. Shezad, M., Liu, X., Feng, S., Kan, X., Shehzad, T. J., Mudassir, A., Wang, W., & Liu, C. (2020). Investigating the co-substitution impact of yttrium–nickel cations on lattice, morphological and magnetic parameters of SrM based ceramics. Ceramics International, 46(7), 8918–8927. https://doi.org/10.1016/j.ceramint.2019.12.138
44. Singh, V. P., Kumar, G., Kumar, A., Rai, R. S., Valente, M. A., Batoo, K. M., Kotnala, R. K., & Singh, M. (2016). Structural, magnetic and Mössbauer study of BaLaxFe12-xO19 nanohexaferrites synthesized via sol-gel auto-combustion technique. Ceramics International, 42(4), 5011–5017. https://doi.org/10.1016/j.ceramint.2015.12.014
45. Slimani, Y., Güngüneş, H., Nawaz, M., Manikandan, A., El Sayed, H. S., Almessiere, M. A., Sözeri, H., Shirsath, S. E., Ercan, I., & Baykal, A. (2018). Magneto-optical and microstructural properties of spinel cubic copper ferrites with Li-Al co-substitution. Ceramics International, 44(12), 14242–14250. https://doi.org/10.1016/j.ceramint.2018.05.028
46. Su, K., Yuan, K., Guo, Z., & He, Y. (2022). Structure and Magnetic Studies of Gadolinium Doped M-type Barium Hexagonal Ferrite. Transactions on Metals and Alloys, 1(1), 1–8. https://doi.org/10.23977/trama.2022.010101
47. Sutka, A., & Mezinskis, G. (2012). Sol-gel auto-combustion synthesis of spinel-type ferrite nanomaterials. Frontiers of Materials Science, 6(2), 128–141. https://doi.org/10.1007/s11706-012-0167-3
48. Taneja, S., Chahar, D., Thakur, P. and Thakur, A. (2021). Influence of bismuth doping on structural, electrical, and dielectric properties of Ni–Zn nanoferrites, J. Alloys Compd., vol. 859, p. 157760, doi: 10.1016/j.jallcom.2020.157760.
49. Tchouank Tekou Carol, T., Sharma, J., Mohammed, J., Kumar, S., & Srivastava, A. K. (2017). Effect of temperature on the magnetic properties of nano-sized M-type barium hexagonal ferrites. AIP Conference Proceedings, 1860. https://doi.org/10.1063/1.4990307
50. Trukhanov, A. V., Trukhanov, S. V., Kostishyn, V. G., Panina, L. V., Korovushkin, V. V., Turchenko, V. A., Vinnik, D. A., Yakovenko, E. S., Zagorodnii, V. V., Launetz, V. L., Oliynyk, V. V., Zubar, T. I., Tishkevich, D. I., & Trukhanova, E. L. (2018). Correlation of the atomic structure, magnetic properties and microwave characteristics in substituted hexagonal ferrites. Journal of Magnetism and Magnetic Materials, 462, 127–135. https://doi.org/10.1016/j.jmmm.2018.05.006
51. V.G., K., Yu., M. A., A.V., T., R.I., S., I.M., I., G.A., S., & A.I., R. (2022). Characterization of c-oriented BaFe12O19 films synthesized by ion beam deposition on Al2O3 (102) substrate. Materials Today Communications, 31(November 2021), 103804. https://doi.org/10.1016/j.mtcomm.2022.10380

4

52. Xu, Y., Yang, G. L., Chu, D. P., and Zhai, H. R. (1990). Theory of the Single Ion Magnetocrystalline Anisotropy of 3d Ions, Phys. Status Solidi, vol. 157, no. 2, pp. 685–693, doi: 10.1002/pssb.2221570221.
53. Yassine, R., Abdallah, A. M., Awad, R., & Bitar, Z. (2022). Structural, optical and magnetic properties of (x)NiO/(1-x)CdFe2O4 nanocomposites. Physica B: Condensed Matter, 624(May 2021), 413444. https://doi.org/10.1016/j.physb.2021.413444
54. Yousaf, M., Nazir, S., Hayat, Q., Akhtar, M. N., Akbar, M., Lu, Y., Noor, A., Zhang, J. M., Shah, M. A. K. Y., & Wang, B. (2021). Magneto-optical properties and physical characteristics of M-type hexagonal ferrite (Ba1-xCaxFe11.4Al0.6O19) nanoparticles (NPs). Ceramics International, 47(8), 11668–11676. https://doi.org/10.1016/j.ceramint.2021.01.006
55. Zhou, X., Zhou, K., Zhang, T., Fan, L., Zhang, H., & Zheng, H. (2021). Static magnetic, complex dielectric and complex permeability properties of aluminum substituted hexagonal barium ferrites based on doping concentration. Journal of the Ceramic Society of Japan, 129(9), 2–9.